REGULAR ARTICLE

Gaussian basis sets for use in correlated molecular calculations. VII. Valence, core-valence, and scalar relativistic basis sets for Li, Be, Na, and Mg

Brian P. Prascher · David E. Woon ·
Kirk A. Peterson · Thom H. Dunning Jr ·
Angela K. Wilson

Abstract Correlation consistent basis sets of double-ζ through quintuple-ζ quality for the alkali and alkaline earth metals Li, Be, Na, and Mg have been developed, including the valence (cc-pVnZ), augmented valence (aug-cc-pVnZ), core-valence (cc-pCVnZ), and weighted core-valence (cc-pwCVnZ) basis sets. The basis sets are also re-contracted for Douglas–Kroll scalar relativistic calculations and are found to be superior to non-relativistic basis sets in recovering scalar relativistic effects. CCSD(T) computations have been performed with these basis sets, and a series of properties have been examined, including atomic ionization potentials and electron affinities, optimized molecular geometries, harmonic vibrational frequencies, atomization energies, and enthalpies of formation for the molecules Li_2, LiF, BeO, BeF, BeH_2, BeF_2, Na_2, NaF, MgO, MgF, MgH_2, and MgF_2.

B. P. Prascher · A. K. Wilson (✉)
Center for Advanced Scientific Computing and Modeling
(CASCaM), Department of Chemistry,
University of North Texas, 1155 Union Circle #305070,
Denton, TX 76203-5070, USA
e-mail: akwilson@unt.edu

D. E. Woon · T. H. Dunning Jr
Department of Chemistry, University of Illinois
at Urbana-Champaign, Urbana, IL 61801, USA

K. A. Peterson (✉)
Department of Chemistry, Washington State University,
Pullman, WA 99164-4630, USA
e-mail: kipeters@wsu.edu

1 Introduction

In ab initio studies of the electronic structure of molecules, exact solution of the non-relativistic Schrödinger equation requires (1) a complete N-electron treatment and (2) a complete one-electron expansion (basis set). The former can be achieved through a full configuration interaction (full CI) calculation, which is rarely applicable to any but the smallest of electronic systems (i.e., typically less than about ten correlated electrons for basis sets of double-zeta quality). Even in small systems where full CI can be applied, the use of modest-sized basis sets is a limiting factor in achieving the exact solution of the Schrödinger equation since the full CI method scales factorially with the number of basis functions. Further, the use of a complete basis set is infeasible, as such sets contain an infinite number of functions. In a practical sense, only approximate solutions to the Schrödinger equation are obtainable, and for the modeling of any system the N-electron and one-electron treatments must be chosen considering both the desired level of accuracy and available computational resources.

The most straightforward strategy for approximating the exact solution to the Schrödinger equation is to first select as large a basis set as possible. However, this quickly limits both the molecular system size and the N-electron treatment that can be employed. The correlation consistent, polarized valence basis sets [cc-pVnZ, where n is the cardinal number of the basis set: D(2), T(3), Q(4), etc.][1–8] have been designed so that post-Hartree-Fock ab initio methods systematically recover the correlation energy as

the basis set size increases. The result of this unique construction is that it enables the complete basis set (CBS) limit to be approached monotonically as the basis set size is increased [1]. This monotonic behavior can be modeled with one of several empirical functions [9–14] to calculate the asymptotic energy, which is an estimate of the CBS limit. Formally, the CBS limit is defined as the limit at which no further improvements in the basis set can be made, and any difference between the CBS limit energy and the exact (experimental) energy is error due solely to the choice of N-electron (and relativistic) treatment. Thus, the correlation consistent basis sets also provide a way to gauge the intrinsic error of ab initio methods [15, 16].

Correlation consistent basis sets have now been developed for most of the p-block atoms, including all-electron basis sets for the first three rows (H–He, B–Ne, Al–Ar, Ga–Kr)[1–8, 17] and pseudopotential (PP) basis sets for the third through fifth rows (Ga-Kr, In-Xe, Tl–Rn) [18–20]. Further, a family of all-electron correlation consistent basis sets has been developed for the $3d$ transition metals (Sc-Zn),[21, 22] while PP-based sets have been reported for the heavier transition metals (Y-Cd, Hf–Hg) [23–25]. There are several families of correlation consistent basis sets beyond the standard valence sets. Examples include the tight d basis sets for inner valence correlation in second row, p-block atoms [cc-pV($n + d$)Z];[2] augmented basis sets for long range interactions and electron affinities [aug-cc-pVnZ]; core-valence basis sets for sub-valence correlation energy (cc-pCVnZ for core-core and core-valence correlation, and cc-pwCVnZ for core-valence correlation);[8, 26, 27] and the Douglas–Kroll-contracted basis sets for the recovery of scalar relativistic effects (cc-pVnZ-DK) [28]. Finally, there has been recent development of correlation consistent basis sets for resolution of the identity (RI) and explicitly correlated F12 methods [29–33].

The present work adds to the suite of available correlation consistent basis sets by providing sets for the s-block atoms Li, Be, Na, and Mg. A preliminary form of the correlation consistent basis sets for s-block atoms through quadruple-ζ quality (developed by some of us)[34, 35] has been available for some time via the Basis Set Exchange [36, 37]. This paper presents slightly modified, final versions where all polarization functions (d, f, g, and h) have been re-optimized using the robust Broyden–Fletcher–Goldfarb–Shanno (BFGS)[38] optimization technique, but also include additional core-valence basis sets and sets contracted for use in relativistic calculations. These new, slightly modified basis sets have already found a niche in benchmarking the correlation consistent Composite Approach (ccCA)[39–43] and studying the ab initio potential energy surfaces of small molecules containing Li, Be, and Mg [44–49].

In the first half of this paper, the construction of correlation consistent basis sets for s-block atoms is discussed, while the second half of the paper is focused on benchmark calculations of atomic and molecular properties utilizing these new basis sets. In particular, double- through quintuple-ζ basis sets are presented for standard valence, tight d valence (for Na and Mg only), diffuse, core-valence, and Douglas–Kroll scalar relativistic computations.

2 General computational considerations

An atomic Hartree–Fock program [50, 51] and the MOLPRO program suite [52] were utilized exclusively for the ab initio computations reported throughout this work. The procedure used in earlier studies [1, 53] for determining the exponents of the basis functions in the correlation consistent basis sets was followed here, i.e., Hartree–Fock (HF) calculations were used to optimize the exponents of the (sp) sets, while configuration interaction calculations with single and double excitations (CISD) were used to optimize the exponents of the higher angular momentum functions ($dfg…$). All CISD-optimized exponents (ζ) in this work were obtained with a BFGS algorithm [38] using double-sided numerical derivatives. The actual optimizations were carried out in the space of $\ln(\zeta)$, and the gradient of the maximum of $\ln(\zeta)$ was converged to better than 1×10^{-6}.

In regard to the molecular benchmark calculations reported and discussed below, the coupled cluster method with single, double, and non-iterative triple excitations, CCSD(T),[54–56] was utilized for energetics. Energy gradients were converged to 10^{-4} E_h/a_o or better in all geometry optimizations, leading to a precision of at least 10^{-7} E_h in total energies. The reported vibrational frequencies and zero-point energy corrections are from harmonic calculations at the CCSD(T)/cc-pVTZ level of theory. Thermochemical values were computed using enthalpies of formation from the National Institute of Standards and Technology (NIST) database [57].

3 Determination of correlation consistent basis sets for Li, Be, Na, and Mg

As in earlier work, the correlation consistent basis sets for Li, Be, Na, and Mg consist of the following: (i) the generally contracted [58] HF orbitals, (ii) additional primitive s- and p-functions taken from the corresponding HF (sp) sets, (iii) spherical harmonic contractions of sets of the higher angular ($dfg…$) functions, and (iv) augmenting functions required to describe either core-valence correlation effects and/or anionic character. The Gaussian functions in (ii)–(iv) were chosen to provide an optimal description of electron correlation.

3.1 cc-pVnZ basis sets

Libraries of HF (sp) primitive sets were determined prior to optimizing the polarization functions for describing correlation effects. These sets were either derived explicitly for this work or taken from Partridge [59]. All s-functions were optimized for the atomic ground states. The p-sets for the Li and Be 2p HF orbitals were optimized for the ^2P ($1s^2 2p$) and ^3P ($1s^2 2s2p$) excited states, respectively. The p-sets for Na and Mg include m primitives optimized for the 2p orbitals in the ground (^2S or ^1S) state and additional n primitives optimized for the 3p orbitals in the appropriate $3s \rightarrow 3p$ excited states analogous to those for Li and Be (^2P for Na; ^3P for Mg). In the discussion which follows, these latter sets are denoted "$(m + n)p$." The coefficients for the first two generally contracted p basis functions (the HF orbitals) in the p-set were determined using two different states: the coefficients for the 2p HF orbitals for Na/Mg were taken from the ($^2S/^1S$) calculation and those for the 3p HF orbital from the ($^2P/^3P$) calculations.

Valence correlating functions cannot be obtained from atomic calculations on Li and Na, as the valence space contains only one electron. Instead, these functions were optimized for Li$_2$ and Na$_2$ in a manner analogous to that adopted for H [1]. A large (sp) set with several of the outermost functions uncontracted was used as a base set, namely, a (16s8p) set of primitive Gaussian functions contracted to [6s5p] for Li, and (20s(10 + 4)p) / [7s6p] set for Na. The interatomic separations were fixed at the experimental values [60] (2.6729 Å for Li$_2$, 3.0788 Å for Na$_2$). The familiar even-tempered parameters (α, β) in

$$\zeta_i = \alpha\beta^{i-1} \quad i = 1, 2, 3, \ldots \tag{1}$$

were then optimized for the CISD energy for the following sequences of polarization functions: (1d), (2d), and (3d) were optimized with the [6s5p] base set; (1f) and (2f) were optimized with the [6s5p3d] set; and (1g) was optimized with the [6s5p3d2f] set, *etc*. The incremental changes in the calculated correlation energy for the ($n\ell$) sets

$$\Delta E_{corr}(n, n - 1) = E corr(n\ell) - E corr[(n - 1)\ell] \tag{2}$$

converge monotonically and can be separated into the usual correlation consistent groupings, (1d), (2d1f), (3d2f1g), (4d3f2g1h), *etc*., which constitute the groups assigned to the cc-pVDZ, cc-pVTZ, cc-pVQZ, and the cc-pV5Z sets, respectively.

The polarization functions for Be and Mg were optimized in CISD calculations on the ground states (^1S) of the atoms. The base sets were (14s8p)/[6s5p] for Be, and (20s(10 + 4)p)/[7s6p] for Mg. Figure 1 plots the corresponding incremental correlation energy lowerings for both the Be and Mg atoms. Polarization functions involving d and higher angular momentum make a much smaller

contribution to the correlation energies of the alkali and alkaline earth metals than they do in the p-block elements. In Li$_2$ and Na$_2$, the (3d2f1g) set recovers just 4.166 and 3.360 mE_h, respectively, beyond the base sets, while in Be and Mg, the (4d3f2g1h) set recovers only an additional 0.633 and 1.069 mE_h, respectively.
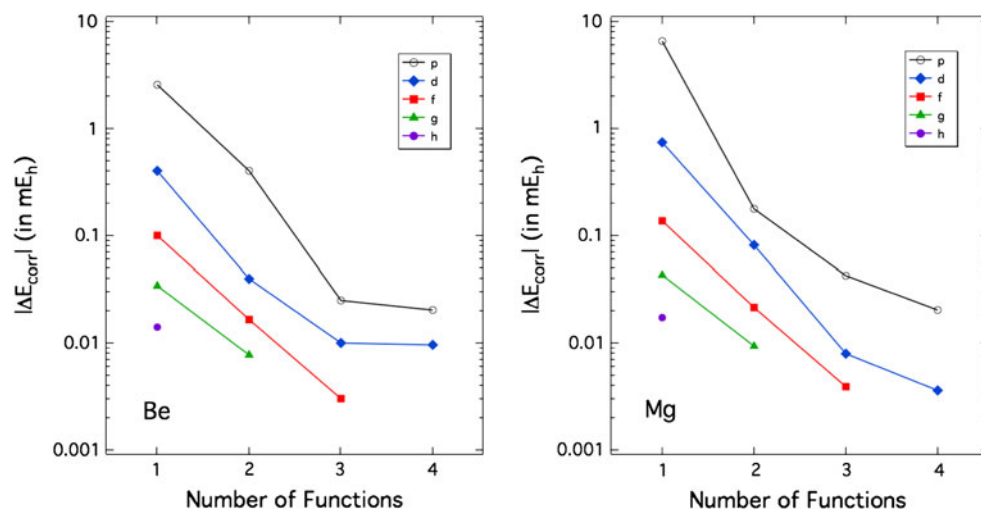
Also shown in Fig. 1 are the incremental correlation contributions due to p-type functions, which utilized [6s1p4d3f2g] and [7s2p4d3f2g] base sets for Be and Mg, respectively. From this figure alone, it appears that p functions are the most important for recovering electron correlation in these elements. However, by utilizing CI calculations that only included configurations describing ns-np near degeneracy effects, e.g., $2s^2$, $2p_x^2$, $2p_y^2$, $2p_z^2$ for Be, more than 90% of the total incremental correlation contributions of the p-type functions shown in Fig. 1 can be attributed to these non-dynamical correlation effects. Hence, the most important angular momentum for dynamical correlation is actually a d-type function as in the p-block elements. As can also be noted in Fig. 1, the typical correlation consistent groupings, i.e., 1d for DZ, 2d1f for TZ, etc., which are also chosen in this work, are not the only choices that could have been made based on these incremental correlation energy lowerings. For example, the first h-type function makes a similar contribution to the correlation energy as the second f- and the third d-type functions and hence could have been included in the cc-pVQZ basis set. In this work, however, we have adopted the same groupings chosen previously for the p-block elements.

Since the valence correlation consistent basis sets determined previously for other elements use the same sp correlating functions as in the HF primitive sets, rather than the optimized ones, (sp) functions to describe (sp) correlation were not explicitly optimized in this study. However, in light of the shifting balance between correlation contributions from polarization and (sp) functions as one moves across the periodic table, the choice of HF sets was reexamined. As in earlier work, the balance of errors in the HF and CISD energies was used to identify the optimum primitive (sp) sets to use in the cc-pVnZ sets.

The selection of s-function sets was straightforward. For Li and Be, the same primitive set sizes adopted for B–Ne proved appropriate with one exception: the (11s) set replaces the (10s) set at the cc-pVTZ level. The Mg sets are the same as those of Al–Ar. In Na, (16s) and (19s) primitive sets replace the smaller sets of s-functions used for Mg–Ar in the cc-pVTZ and cc-pVQZ basis sets, respectively.

The selection of p-function sets was also straightforward. Again, the primitive sets for Be match those of B–Ne, but larger p-sets were adopted for Na and Mg than for Al–Ar. This is largely due to the manner in which the

Fig. 1 Incremental correlation energy lowerings at the frozen core CISD level of theory as a function of polarization function type for the Be and Mg atoms

functions are used to describe the atomic ground and excited states as described above. The p-sets for Li are the same as those selected for Be–Ne, but a slightly unusual base set was employed in making this determination—the fifth and sixth primitives of the $(8p)$ primitive set were uncontracted in order to improve the description of the ^2P HF wave function.

Table 1 summarizes the compositions of the valence correlation consistent basis sets determined for Li, Be, Na, and Mg and compares them to those of B–Ne and Al–Ar. The sizes of the contracted sets are the same for each row. It should be noted that the final cc-pVnZ basis sets were obtained by re-optimizing all of the polarization exponents in the presence of the cc-pVnZ [sp] sets.

3.2 aug-cc-pVnZ basis sets

With cc-pVnZ sets defined, the second subject of interest is the large r region of basis function space, where additional

diffuse character is often necessary for accurately describing electron affinities, electric field response properties such as permanent electrical moments and polarizabilities, and long-range interactions. We have again chosen to optimize diffuse functions for the negative ions, but these exponents also work well for response properties. The optimization strategy follows that of previous work [17, 53] with small differences. One exponent is added for each symmetry present in the standard valence basis set. The exponents of lowest angular momentum (usually s and p) are optimized for the anion HF energy, while the higher ℓ functions are optimized for the anion CISD energy. Here, the nature of Li and Na forces shifting the optimization of the p exponents to the CISD step. Also, since Be and Mg will not bind an additional electron, the exponents of the diffuse functions for these atoms have been optimized in calculations on their hydrides (BeH$^-$ and MgH$^-$), a strategy also adopted by Spitznagel et al. [61]. The Be–H and Mg–H distances were frozen at 1.442 Å and 1.953 Å,

Table 1 Summary of correlation consistent polarized valence (cc-pVnZ) basis set dimensions for the first and second row atoms Li through Ar

Basis set	Primitive HF sets			Contr. sets	Pol. Set	Size[a]
	Li	Be	B–Ne			
cc-pVDZ	$(9s4p)$	$(9s4p)$	$(9s4p)$	$[3s2p]$	$(1d)$	14
cc-pVTZ	$(11s5p)$	$(11s5p)$	$(10s5p)$	$[4s3p]$	$(2d1f)$	30
cc-pVQZ	$(12s6p)$	$(12s6p)$	$(12s6p)$	$[5s4p]$	$(3d2f1g)$	55
cc-pV5Z	$(14s8p)$	$(14s8p)$	$(14s8p)$	$[6s5p]$	$(4d3f2g1h)$	91
	Na	Mg	Al–Ar			
cc-pVDZ	$(12s(6+2)p)$	$(12s(6+2)p)$	$(12s8p)$	$[4s3p]$	$(1d)$	18
cc-pVTZ	$(16s(7+3)p)$	$(15s(7+3)p)$	$(15s9p)$	$[5s4p]$	$(2d1f)$	34
cc-pVQZ	$(19s(8+4)p)$	$(16s(8+4)p)$	$(16s11p)$	$[6s5p]$	$(3d2f1g)$	59
cc-pV5Z	$(20s(10+4)p)$	$(20s(10+4)p)$	$(20s12p)$	$[7s6p]$	$(4d3f2g1h)$	95

[a] Size of contracted sets assuming pure spherical harmonic ($dfgh$) functions (5d, 7f, etc.)

respectively, and the corresponding aug-cc-pVnZ sets were used for H. It should be noted that the negative charge resides on the metal in these molecules.

3.3 cc-pV(n + d)Z basis sets

For second row atoms (Al–Ar), previous studies have shown that an additional tight d function for each basis set is important in accelerating the convergence of bond lengths and dissociation energies [62–69]. This phenomenon has been investigated in SO_2,[62–64, 67] $HSO \leftrightarrow HOS$ isomerization,[68, 69] and in silicon molecules [65, 70]. After noting large differences between the dissociation energies of SO_2 using the standard cc-pVnZ basis sets, as compared with the cc-pwCVnZ basis sets, it was found that adding an additional tight d function and reoptimizing the d primitives resulted in markedly improved dissociation energies relative to experiment [67].

The construction of cc-pV(n + d)Z basis sets follows the prescription previously described [2]. Specifically for the cc-pV(n + d)Z basis sets, a single tight (large exponent) d function was added to the double-, triple-, quadruple-, and quintuple-ζ cc-pVnZ basis sets. All of the d functions at each basis set level were then reoptimized in CISD calculations using the Na_2 and the MgH ($r = 1.7302$ Å) molecules. The exponents of the cc-pVnZ and cc-pV(n + d)Z basis sets are plotted in Fig. 2 for comparison. It can be seen from the figure that there is little change in the original valence functions upon optimization with a tight d function, and that the additional d function moves to describe more of the inner valence space with increasing basis set size.
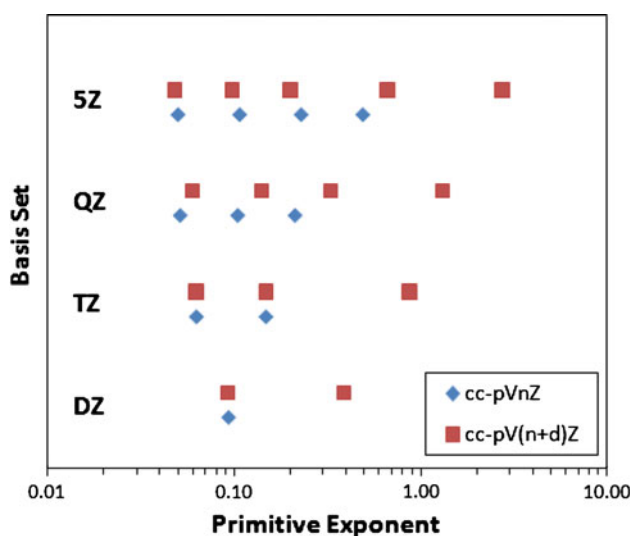

Fig. 2 A comparison of the d function exponents in the cc-pVnZ and cc-pV(n + d)Z basis sets of Na

3.4 cc-pCVnZ and cc-pwCVnZ basis sets

Two strategies have been previously introduced by which the standard correlation consistent valence basis sets (cc-pVnZ) could be extended in a systematic manner to account for core and core-valence correlation contributions. These sets, designated cc-pCVnZ and cc-pwCVnZ, exploit the consistency observed in the description of the correlation energy for the inner shell electrons, and exhibit similar convergence behavior to the valence sets. Groups of functions were added to the sequence of valence sets and, in the cc-pCVnZ case, optimized for the difference in correlation energy between valence electrons and valence plus outer-core electrons (*i.e.*, the sum of the core-core and core-valence correlation energies was minimized). The "weighted" core-valence basis sets, cc-pwCVnZ, differ in this latter regard by biasing the optimization toward core-valence correlation:

$$E_{opt} = E_{core-valence}^{CISD} + 0.01 \times E_{core-core}^{CISD}. \quad (3)$$

The above procedure was also used for the atoms that are the subject of this work. The "core" sets added to Li and Be are the same as those added to the remainder of the first row: $(1s1p)$ "core" sets are added to the cc-pVDZ set to form the cc-pCVDZ and cc-pwCVDZ sets, $(2s2p1d)$ "core" sets are added to the cc-pVTZ set to form the cc-pCVTZ or cc-pwCVTZ sets, $(3s3p2d1f)$ "core" sets are added to the cc-pVQZ set to form the cc-pCVQZ and cc-pwCVQZ sets, and $(4s4p3d2f1g)$ sets were added to the cc-pV5Z. For Na and Mg (and the rest of the second row), the "core" sets are larger since the outer-core has grown from $1s^2$ to $2s^2 2p^6$ (correlation of the $1s^2$ electrons of Na and Mg is not included). So for the second row atoms, $(1s1p1d)$ is added to the cc-pVDZ set, $(2s2p2d1f)$ to the cc-pVTZ, and $(3s3p3d2f1g)$ to the cc-pVQZ set to form the corresponding core-valence basis sets. To avoid near linear-dependence in the s functions at the quintuple-ζ level for Na and Mg, an additional four s functions are uncontracted from the Hartree–Fock set and take the place of the usual optimized tight s functions for core-valence correlation. In addition, the basis set contraction representing the HF $3s$ orbital is then redundant and has been deleted, i.e., the $20s14p$ primitive set was recontracted to $10s6p$. An optimized set of $4p4d3f2g1h$ tight functions are then added. In all cases the functions in each of the "core" sets were optimized in the presence of the corresponding valence set. Atomic HF energies were used in the optimizations for the valence energies of Li and Na, while CISD energies were used for the remaining quantities. It should be noted that the resulting cc-pCVnZ basis sets are very similar to the CVnZ sets reported previously by Iron et al. [71].

Figure 3 compares the resulting cc-pCVnZ and cc-pwCVnZ exponents for the Na atom. Particularly for the
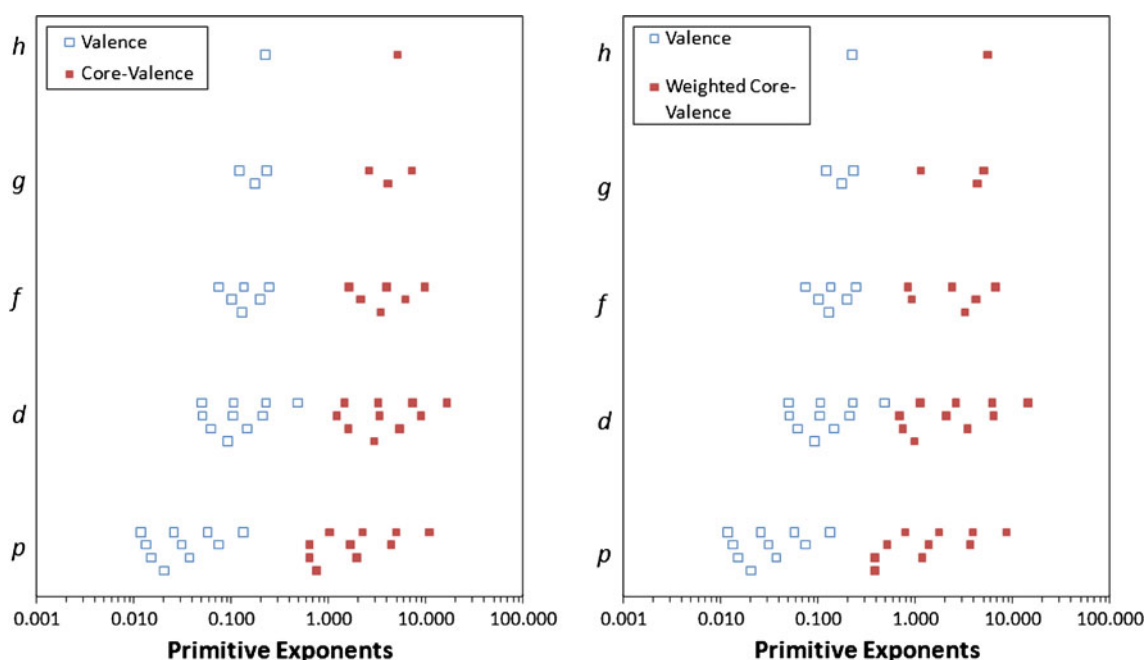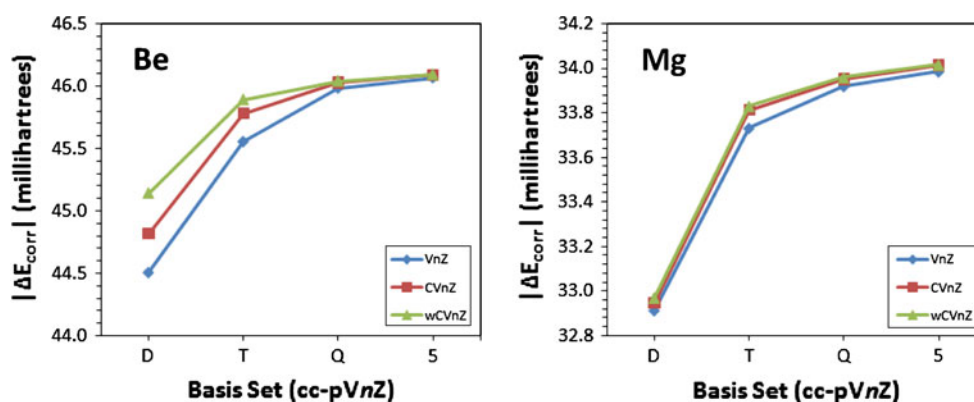
Fig. 3 Plots of the exponents for the valence (cc-pVnZ) versus core-valence (cc-pCVnZ) and weighted core-valence (cc-pwCVnZ) functions of the Na atom, grouped by angular momentum

Fig. 4 Valence correlation energies recovered by the valence (VnZ), core-valence (CVnZ), and weighted core-valence (wCVnZ) basis sets from CCSD(T) calculations

functions of *dfgh* symmetry, the cc-pwCVnZ exponents are considerably more diffuse than the tight functions of the cc-pCVnZ series since the latter are more strongly influenced by the contributions of core-core correlation. Particularly in the cases of Li and Be, the more diffuse nature of the cc-pwCVnZ exponents leads to larger contributions to the valence correlation energy than the cc-pCVnZ basis sets, although both lead to lower valence correlation energies compared to just the cc-pVnZ basis sets as shown in Fig. 4 for Be and Mg.

Figure 5 demonstrates the necessity of using basis sets designed for core-core and core-valence correlation by comparing the CCSD correlation energies recovered by the valence and core-valence basis sets. Compared to either family of core-valence basis sets, the valence sets (cc-pVnZ) obviously provide a very inadequate description of

core correlation effects. Even use of the cc-pV5Z basis set results in 20 mE_h less core-core correlation energy than the cc-pCV5Z results for Li and Be with differences of more than 100 mE_h in Na and Mg. Figure 5 also demonstrates the difference in construction of the cc-pCVnZ and cc-pwCVnZ basis sets, namely that the former recover more core-core correlation energy, while the latter recover a greater fraction of the core-valence correlation energy but with a resulting slower convergence of the core-core contribution. For example, in calculations on Na, the smaller cc-pwCVDZ basis set recovers about the same amount of *core-valence* correlation energy as the larger cc-pCVTZ basis set, the cc-pwCVTZ basis set recovers nearly the same amount as the cc-pCVQZ basis set, etc. The faster convergence of the core-valence correlation energy has been shown to be beneficial in calculating the effects of
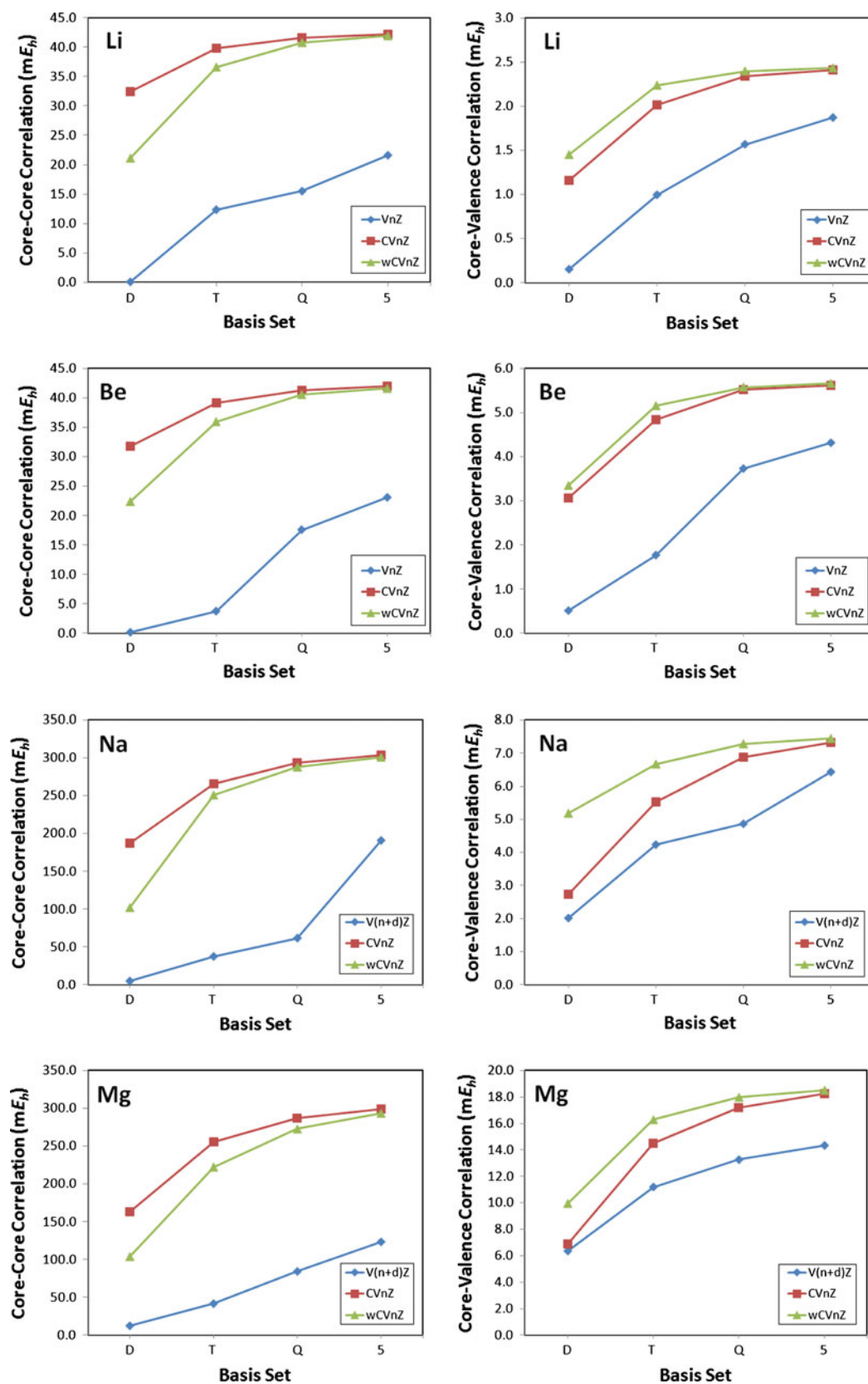
Fig. 5 Core-core and core-valence correlation energies computed with the CCSD method and the valence (V*n*Z), core-valence (CV*n*Z) and weighted core-valence (wCV*n*Z) basis sets (the 1*s* electrons of Na and Mg are not correlated)

core correlation on dissociation energies and spectroscopic properties. However, in cases where a more accurate description of core-core correlation might be important or when the lowest possible correlation energies are of interest, the cc-pCVnZ basis sets should be employed. Both core-valence basis sets do, however, converge to the same CBS limits.

3.5 Recontracted basis sets for Douglas–Kroll scalar relativistic computations

The necessity of systematically altering a basis set to accommodate a relativistic Hamiltonian has been discussed for first, second, and third row p-block atoms and molecules by de Jong et al. [28] with regard to the Douglas–Kroll (DK) Hamiltonian. The problem in using basis sets contracted with non-relativistic methods is the improper description of the radial contraction that occurs in core s- and p-type orbitals. Specifically, atomic contractions optimized with non-relativistic HF produce core s and p orbitals that are too diffuse. The use of these diffuse core orbitals results in DK energies that are too high. The investigation by de Jong et al. demonstrated that by

recontracting the correlation consistent basis sets in calculations with the DK Hamiltonian, the scalar relativistic energy recovered with each basis set level is significantly improved.

In this study, we introduce a similar set of DK-contracted basis sets for Li, Be, Na, and Mg, denoted cc-pVnZ-DK, aug-cc-pVnZ-DK, etc. These were obtained by carrying out HF calculations with the DK Hamiltonian utilizing a fully uncontracted basis set. The resulting atomic orbital coefficients are then employed as contraction coefficients just as in the non-relativistic case described above. Figure 6 plots the scalar relativistic effects on the HF energy as calculated with the DK Hamiltonian with both the non-relativistic-contracted cc-pVnZ and DK-contracted cc-pVnZ-DK basis sets. While the differences between cc-pVnZ and cc-pVnZ-DK are small for both Li and Be (less than 0.1 mE_h), the convergence behavior of the scalar relativistic effect is markedly different between the two sets. In particular, the cc-pVnZ-DK sets are well converged at the TZ level while the calculated relativistic correction actually decreases with basis set size when the non-relativistic cc-pVnZ basis sets are used. In the cases of Na and Mg, both series of basis sets are seemingly well
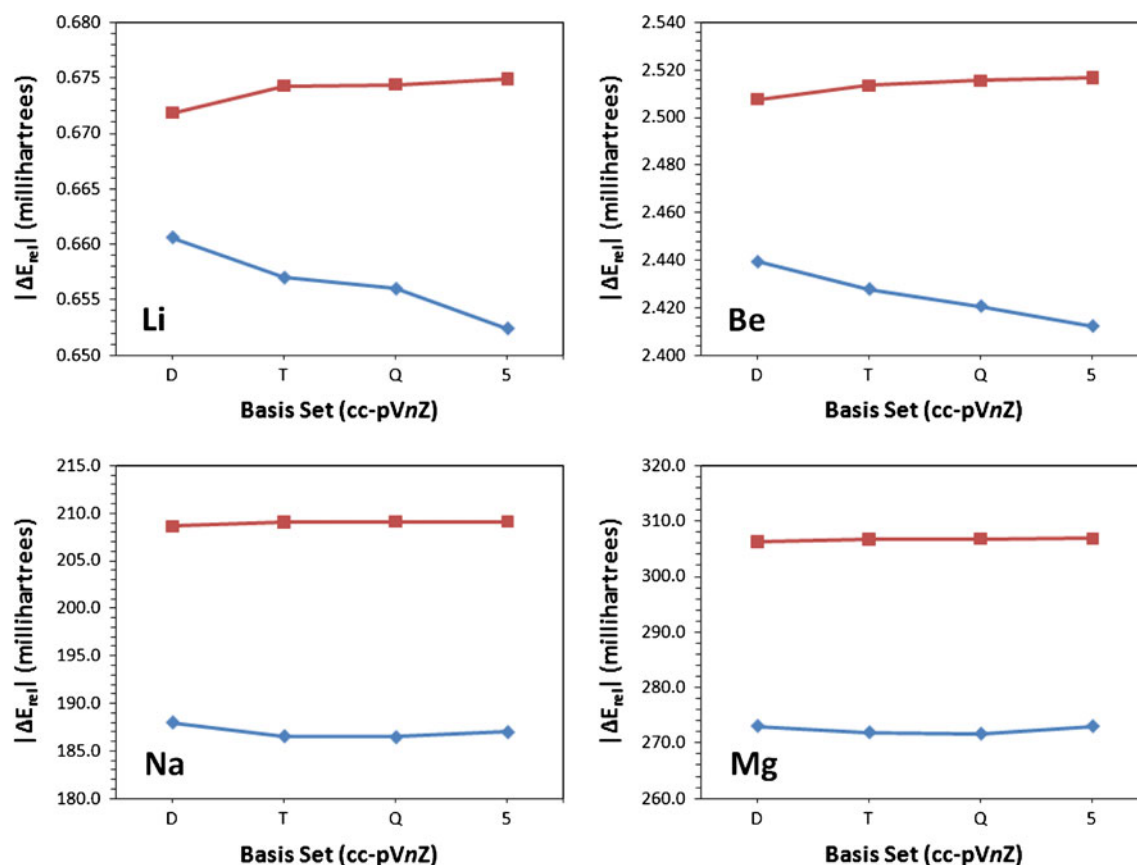

Fig. 6 Comparisons of the Douglas–Kroll (DK) scalar relativistic corrections to the atomic non-relativistic Hartree–Fock energy using the original cc-pVnZ (*diamonds*) and cc-pVnZ-DK (*squares*) basis sets as a function of increasing basis set size

converted at the TZ level, but the cc-pVnZ sets strongly underestimate the total scalar relativistic effects on the HF energy by 20-30 mE_h, making them unreliable for use in DK calculations. It should perhaps also be noted that the use of the DK-contracted sets in non-relativistic calculations exhibit unacceptable HF errors, e.g., about 0.1 mE_h for Be in the triple-zeta basis set.

4 Atomic and molecular properties

4.1 Ionization potentials and electron affinities

To demonstrate the ability of the correlation consistent basis sets to correctly describe the frontier orbital properties of the alkali and alkaline earth metal atoms, ionization potentials and electron affinities have been computed at the CCSD(T) level of theory and are listed in Table 2. Due to the one electron valence of Li and Na, the frozen-core ionization potentials are the same as the HF computed values, and it is seen that there is very little difference between successive ζ-levels. Further, comparing the Li and Na aug-cc-pV5Z ionization potentials with experiment

shows errors of 0.050 and −0.188 eV, respectively. It is only when core-valence correlation is included that the ionization potentials of these two atoms compare well with experiment. Even at the cc-pCVDZ level, for example, the addition of core correlation is enough to bring the Li ionization potential within 0.04 eV of experiment. Using the cc-pwCVDZ basis set instead of the cc-pCVDZ set makes a larger impact on the computed ionization potentials of Li, Be, Na, and Mg. For example, employing the cc-pCVDZ basis set in computing the Li ionization potential shows an error relative to experiment of 0.036 eV, but the cc-pwCVDZ basis set shows an error of 0.027 eV. This observation is typical for the rest of the atomic ionization potentials of Table 2: the cc-pwCVnZ basis sets give results closer to the experimental value when compared with the cc-pCVnZ basis sets. Further, it has been remarked previously that both basis sets will converge on the same CBS limit for properties of interest, and we show that to be true for the atoms of this work. The electron affinities of Be and Mg are not reported since these atoms do not bind an electron.

The use of diffuse functions in the computation of anionic properties is vital to achieving results that compare

Table 2 Ionization potentials and electron affinities (eV) of the alkali and alkaline earth metals from CCSD(T) calculations

Basis[a]	Li		Be		Na		Mg	
	IP	EA	IP$_1$	IP$_2$	IP	EA	IP$_1$	IP$_2$
cc-pVDZ	5.342	0.414	9.290	18.086	4.951	0.406	7.521	14.711
cc-pVTZ	5.342	0.480	9.285	18.124	4.952	0.437	7.527	14.721
cc-pVQZ	5.342	0.569	9.296	18.125	4.951	0.523	7.531	14.722
cc-pV5Z	5.342	0.580	9.298	18.125	4.951	0.522	7.533	14.722
aug-cc-pVDZ	5.342	0.592	9.287	18.091	4.952	0.526	7.523	14.711
aug-cc-pVTZ	5.342	0.615	9.286	18.124	4.952	0.544	7.528	14.721
aug-cc-pVQZ	5.342	0.617	9.296	18.125	4.951	0.545	7.531	14.722
aug-cc-pV5Z	5.342	0.617	9.299	18.125	4.951	0.545	7.533	14.722
cc-pCVDZ	5.356	0.474	9.273	18.145	5.000	0.444	7.542	14.793
cc-pCVTZ	5.379	0.481	9.303	18.192	5.077	0.442	7.598	14.934
cc-pCVQZ	5.388	0.570	9.316	18.205	5.114	0.527	7.619	14.982
cc-pCV5Z	5.390	0.581	9.319	18.207	5.127	0.526	7.630	15.002
cc-pwCVDZ	5.365	0.476	9.278	18.154	5.092	0.443	7.567	14.869
cc-pwCVTZ	5.386	0.482	9.309	18.199	5.113	0.443	7.613	14.975
cc-pwCVQZ	5.390	0.570	9.318	18.207	5.127	0.527	7.627	15.001
cc-pwCV5Z	5.391	0.581	9.320	18.208	5.131	0.526	7.633	15.008
aug-cc-pwCVDZ	5.365	0.610	9.277	18.157	5.094	0.539	7.571	14.872
aug-cc-pwCVTZ	5.386	0.615	9.310	18.199	5.114	0.543	7.613	14.976
aug-cc-pwCVQZ	5.390	0.617	9.318	18.207	5.127	0.547	7.628	15.001
aug-cc-pwCV5Z	5.391	0.617	9.320	18.208	5.131	0.548	7.633	15.008
Experiment[b]	5.392	0.618	9.323	18.211	5.139	0.548	7.646	15.035

[a] The cc-pV(n + d)Z and aug-cc-pV(n + d)Z basis sets have been used for Na and Mg. Only the valence electrons are correlated in the cc-pVnZ and aug-cc-pVnZ calculations, all other calculations correlate the ns, np, $(n − 1)s$, and $(n − 1)p$ electrons

[b] Refs. [77–82] (as cited by Ref. [83])

with experiment. This claim is supported by the fact that, at the cc-pVDZ level, the Li and Na electron affinities are in error by −0.204 and −0.142 eV, respectively. When the diffuse functions are included (aug-cc-pVDZ), the errors in the Li and Na electron affinities drop nearly an order of magnitude to −0.026 and −0.022 eV, respectively. Further, the inclusion of core-valence correlation does not have a significant impact on the electron affinities of Li or Na at the triple-ζ level or higher.

4.2 Optimized geometries and vibrational frequencies

The optimized CCSD(T) geometries of several di- and triatomic molecules and their corresponding harmonic vibrational frequencies computed with the cc-pV(T + d)Z basis set are listed in Table 3. The impact of core-valence correlation is readily seen in the optimized geometries of the diatomics. For example, the bond length of Li_2 (the smallest system of Table 3) at the cc-pV5Z level deviates from experiment by 0.027 Å, while the corresponding core-valence basis set results with all electrons correlated show differences of only 0.002 Å. A similar trend is observed in the bond lengths of LiF, Na_2, NaF, and MgF. A larger than expected difference between theory and experiment is observed for the equilibrium bond length of MgO (0.010 Å) with the aug-cc-pwCV5Z basis set. Experimentally, this system is observed to have low-lying $^1\Pi$ and $^3\Pi$ excited states that complicate the analysis of the rotational-vibrational spectrum of its $^1\Sigma^+$ ground state [72–75]. While the CCSD(T) value shown in Table 3 with the aug-cc-pwCV5Z basis set, 1.738 Å, would normally be expected to have an accuracy of about 0.003 Å by comparison to other species of this table, inspection of the CCSD results for MgO reveals that its T_1 diagnostic [76] is rather large, 0.046, with concomitant large T_1 and T_2 amplitudes of 0.092 and 0.168, respectively. Hence, non-dynamical correlation should play a role in the ground state of MgO, which decreases the reliability of CCSD(T) in this case and leads to the larger than expected error with respect to the accurate experimental value. Note that this is independent of any interactions with the low-lying $^1\Pi$ and $^3\Pi$ states that plague the experimental work. Similar results have been reported by Iron et al. [71] with the CVnZ basis sets for several of the diatomic molecules of this study.

Another basis set effect that is observed is the general improvement in the convergence of the bond lengths with the cc-pV(n + d)Z basis sets relative to the cc-pVnZ basis sets. The largest tight d effects observed are in the bond lengths of MgO and MgF. Using the cc-pVDZ basis set, the bond lengths of MgO and MgF are 1.774 and 1.773 Å, respectively, which decrease to 1.753 and 1.756 Å, respectively, when the cc-pV(D + d)Z basis set is used. At the higher ζ-levels, the changes in the bond length due to

the tight d function are less than 0.01 Å. A similar effect due to the tight d function is seen in the aug-cc-pVDZ/aug-cc-pV(D + d)Z bond lengths of MgO and MgF, and in the cc-pVDZ/cc-pV(D + d)Z bond lengths of MgF_2.

4.3 Thermochemistry

The atomization energies and enthalpies of formation for a set of twelve s-block molecules have been computed. The ΣD_0 values are given in Table 4 (along with the zero-point energy corrections computed at the CCSD(T)/cc-pVTZ level of theory), while the ΣD_e energies, enthalpies of formation, and thermal corrections are reported in the supplemental material. The rest of this discussion is with regard to the atomization energies alone. The desired accuracy of both the computed atomization energies and enthalpies of formation with respect to experiment is ± 1.0 kcal/mol. However, it should be noted that this is complicated in the present cases by large experimental uncertainties in the atomization energies as shown in Table 4.

It is readily seen that the computed cc-pVTZ (and higher) atomization energies of Li_2 and Na_2 are within 1.0 kcal/mol of their respective experimental values; the atomization energies of BeO and NaF are also within 1.0 kcal/mol of experiment at the cc-pV5Z level. The net effect of including diffuse functions in the computed atomization energies is to reduce the error with respect to experiment in each of the molecules studied—most notably in those systems with an electronegative element: LiF, BeO, BeF, NaF, MgO, MgF, BeF_2, and MgF_2. Presumably this has more to do, however, with including diffuse functions on oxygen or fluorine than the use of aug-cc-pVnZ sets on the metal. Despite this observation, utilizing the aug-cc-pVnZ basis sets does not result in 1.0 kcal/mol accuracy with respect to experiment in all of the computed atomization energies (at least in the cases where the experimental uncertainties are small enough to make this distinction). For example, LiF, BeF, BeF_2, and MgF_2 still suffer differences greater than 1.0 kcal/mol from their experimental atomization energies. In the cases of MgO and BeH_2, the best CCSD(T) results shown in Table 4 differ from their experimental values by about 10 kcal/mol or more. In both cases, the experimental values are rather uncertain, especially for BeH_2. In the case of MgO the deviation from experiment can also be partly attributed to intrinsic errors of the CCSD(T) method, i.e., the large T_1 diagnostic as discussed above. In contrast, the T_1 diagnostic for BeH_2 is small and less than 0.005.

The inclusion of core-valence correlation is important in achieving sub-kcal/mol accuracy, and as shown in Table 4 its contribution to the atomization energies can be on the order of 1 kcal/mol or greater. For example, the difference

Table 3 Optimized bond lengths (Å) and triple-ζ frequencies (ω_e in cm^{-1}) of s-block di- and triatomic molecules from CCSD(T) calculations with various families of correlation consistent basis sets

Molecule	ζ	VnZ[a]	V(n + d)Z[a]	aVnZ[a]	aV(n + d)Z[a]	CVnZ[b]	wCVnZ[b]	aCVnZ[b]	awCVnZ[b]	Expt.
Li$_2$	D	2.731	–	2.727	–	2.699	2.701	2.700	2.702	
	T	2.701	–	2.701	–	2.680	2.677	2.680	2.677	
	Q	2.699	–	2.699	–	2.676	2.674	2.676	2.674	
	5	2.699	–	2.699	–	2.674	2.674	2.674	2.674	2.6729[c]
	ω_e	346.5	–	346.7	–	353.0	355.4	353.4	354.2	351.43[c]
LiF	D	1.592	–	1.606	–	1.579	1.556	1.596	1.587	
	T	1.588	–	1.591	–	1.572	1.557	1.574	1.568	
	Q	1.578	–	1.582	–	1.564	1.561	1.567	1.565	
	5	1.580	–	1.581	–	1.565	1.563	1.565	1.564	1.563864[c]
	ω_e	904.1	–	887.4	–	905.6	937.5	894.1	908.6	910.34[c]
BeO	D	1.369	–	1.370	–	1.365	1.357	1.366	1.361	
	T	1.344	–	1.346	–	1.338	1.333	1.341	1.336	
	Q	1.338	–	1.339	–	1.331	1.330	1.333	1.331	
	5	1.337	–	1.337	–	1.331	1.330	1.331	1.330	1.3309[c]
	ω_e	1458.4	–	1451.7	–	1468.0	1477.6	1458.7	1466.1	1487.32[c]
BeF	D	1.413	–	1.414	–	1.409	1.399	1.407	1.397	
	T	1.371	–	1.374	–	1.365	1.359	1.369	1.365	
	Q	1.367	–	1.369	–	1.361	1.359	1.363	1.362	
	5	1.367	–	1.368	–	1.361	1.360	1.362	1.361	1.3610[c]
	ω_e	1260.7	–	1242.4	–	1270.2	1280.0	1248.1	1256.6	1247.36[c]
Na$_2$	D	3.207	3.205	3.204	3.203	3.163	3.113	3.148	3.095	
	T	3.178	3.180	3.178	3.179	3.095	3.088	3.083	3.081	
	Q	3.178	3.179	3.178	3.179	3.087	3.080	3.087	3.080	
	5	3.179	3.179	3.179	3.179	3.083	3.079	3.073	3.081	3.0788[c]
	ω_e	151.5	152.4	151.5	152.5	159.4	161.9	159.7	161.1	159.124[c]
NaF	D	1.934	1.928	1.986	1.982	1.910	1.899	1.950	1.938	
	T	1.980	1.971	1.996	1.990	1.928	1.919	1.939	1.934	
	Q	1.989	1.982	1.994	1.990	1.928	1.923	1.931	1.928	
	5	1.989	1.987	1.991	1.989	1.928	1.926	1.928	1.927	1.92594[c]
	ω_e	548.7	554.9	532.3	536.4	543.6	554.9	524.9	530.8	536[c]
MgO	D	1.774	1.753	1.786	1.770	1.768	1.753	1.774	1.764	
	T	1.759	1.752	1.766	1.759	1.743	1.736	1.748	1.743	
	Q	1.756	1.753	1.759	1.755	1.739	1.737	1.741	1.740	
	5	1.754	1.753	1.755	1.754	1.738	1.737	1.739	1.738	1.74817[l]
	ω_e	782.1	796.5	770.9	781.7	805.3	817.5	794.2	802.6	785.22[l]
MgF	D	1.773	1.756	1.785	1.775	1.771	1.762	1.776	1.771	
	T	1.768	1.760	1.777	1.769	1.754	1.746	1.761	1.755	
	Q	1.766	1.762	1.770	1.766	1.751	1.748	1.753	1.752	
	5	1.765	1.764	1.766	1.765	1.751	1.750	1.751	1.751	1.7500[c]
	ω_e	722.9	723.2	698.5	702.1	726.0	731.5	702.0	710.2	711.69[c]
BeH$_2$	D	1.339	–	1.340	–	1.336	1.333	1.336	1.336	
	T	1.334	–	1.333	–	1.330	1.327	1.330	1.328	
	Q	1.331	–	1.331	–	1.326	1.326	1.327	1.326	
	5	1.331	–	1.331	–	1.326	1.326	1.326	1.326	1.326407[i]
	$\omega 1_e$	710.3	–	707.9	–	717.9	719.7	715.8	718.6	708.5[e]
	$\omega 2_e$	2030.0	–	2025.4	–	2039.7	2047.4	2032.4	2041.6	
	$\omega 3_e$	2238.7	–	2232.3	–	2249.1	2255.3	2243.1	2250.1	2172.2[e]
BeF$_2$	D	1.417	–	1.417	–	1.412	1.406	1.407	1.402	

Table 3 continued

Molecule	ζ	VnZ[a]	V($n+d$)Z[a]	aVnZ[a]	aV($n+d$)Z[a]	CVnZ[b]	wCVnZ[b]	aCVnZ[b]	awCVnZ[b]	Expt.
	T	1.382	–	1.384	–	1.377	1.372	1.380	1.377	
	Q	1.378	–	1.380	–	1.373	1.372	1.375	1.374	
	5	1.379	–	1.379	–	1.373	1.373	1.374	1.373	
	$\omega 1_e$	335.4	–	336.8	–	344.2	345.9	342.7	344.2	342.61[f]
	$\omega 2_e$	727.1	–	719.7	–	731.4	737.0	722.8	726.4	769.09[f]
	$\omega 3_e$	1584.3	–	1566.2	–	1591.4	1599.1	1568.9	1573.7	1555.05[f]
MgH$_2$	D	1.710	1.707	1.717	1.713	1.707	1.703	1.709	1.706	
	T	1.712	1.710	1.713	1.712	1.700	1.698	1.701	1.698	
	Q	1.711	1.710	1.711	1.710	1.698	1.697	1.698	1.697	
	5	1.710	1.710	1.710	1.710	1.696	1.696	1.697	1.696	1.69582j
	$\omega 1_e$	439.2	434.8	439.0	434.0	457.0	446.2	447.8	442.1	450.4[g]
	$\omega 2_e$	1605.5	1603.4	1595.6	1594.7	1624.5	1620.5	1615.6	1615.2	
	$\omega 3_e$	1632.3	1629.0	1618.6	1618.3	1650.0	1644.2	1637.9	1630.9	1576.8[g]
MgF$_2$	D	1.760	1.744	1.769	1.760	1.756	1.748	1.761	1.756	
	T	1.756	1.749	1.763	1.757	1.743	1.736	1.747	1.742	
	Q	1.754	1.751	1.757	1.754	1.739	1.737	1.741	1.739	
	5	1.753	1.752	1.754	1.753	1.738	1.737	1.739	1.738	
	$\omega 1_e$	156.6	154.7	149.2	145.3	160.0	156.9	155.3	153.7	254[h]
	$\omega 2_e$	571.3	571.0	556.7	558.9	575.5	579.1	561.4	567.0	
	$\omega 3_e$	891.8	890.5	864.8	867.5	896.4	900.8	872.6	879.9	862[h]

[a] Only the ns and np electrons are correlated

[b] The $(n-1)s$ and $(n-1)p$ electrons are correlated in addition to the ns and np

[c] Ref. [60]

[d] Ref. [73]

[e] Ref. [84]

[f] Ref. [85]

[g] Ref. [86]

[h] Ref. [87]

[i] Ref. [88]

[j] Ref. [89]

[k] Ref. [74]

[l] Ref. [75]

between experiment and the aug-cc-pV5Z atomization energy of BeF is 3.8 kcal/mol, which is reduced to 2.7 kcal/mol using the aug-cc-pCV5Z basis set and correlating all the electrons (2.6 kcal/mol using the aug-cc-pwCV5Z basis set). Further, the difference between experiment and the aug-cc-pV5Z atomization energy of MgF$_2$ is 3.1 kcal/mol, which is reduced to 2.1 kcal/mol using the aug-cc-pCV5Z or aug-cc-pwCV5Z basis sets and correlating the $2s2p$ electrons of Mg and the $1s$ of F. Similar observations were also made by Iron et al. [71] for several of the diatomics of Table 4. Including diffuse functions in addition to core-valence correlation has the same net effect of lowering the deviation of computed atomization energies with respect to experiment as including diffuse functions in the standard valence basis sets.

5 Conclusions

Families of correlation consistent basis sets for Li, Be, Na, and Mg have been presented for valence electron calculations. Specifically, new cc-pVnZ and aug-cc-pVnZ basis sets of double-, triple-, quadruple-, and quintuple-ζ quality have been developed and examined. In addition, a set of tight d basis sets, cc-pV($n+d$)Z, have been developed for Na and Mg in correlated valence calculations.

For subvalence correlation, core-valence and weighted core-valence (cc-pCVnZ and cc-pwCVnZ) basis sets have been developed. Calculations of atomic core-valence correlation energies demonstrate the necessity of including core-valence functions when subvalence correlation is needed (i.e. for high accuracy thermochemistry). The cc-pCVnZ and cc-pwCVnZ basis sets converge toward the

Table 4 Atomization energies (ΣD_0 in kcal/mol) of some s-block molecules, computed with the CCSD(T) method and various families of correlation consistent basis sets

Basis[a]	Li$_2$	LiF	BeO	BeF	Na$_2$	NaF	MgO	MgF	BeH$_2$	BeF$_2$	MgH$_2$	MgF$_2$
cc-pVDZ	21.97	121.56	81.14	116.97	15.65	97.80	42.03	91.09	129.88	269.70	90.96	217.85
cc-pVTZ	23.27	130.96	95.89	129.60	16.46	107.55	53.46	101.26	136.33	293.41	98.03	237.56
cc-pVQZ	23.54	135.16	100.77	133.07	16.55	111.40	58.09	105.43	138.31	299.86	99.59	245.33
cc-pV5Z	23.58	136.18	102.48	133.95	16.59	113.01	59.57	106.58	138.69	301.51	99.97	247.27
aug-cc-pVDZ	22.16	129.42	85.16	122.07	15.74	108.76	50.81	101.24	131.89	279.65	94.45	237.16
aug-cc-pVTZ	23.33	133.59	98.12	130.92	16.48	111.47	57.10	104.42	137.00	296.10	98.87	243.05
aug-cc-pVQZ	23.55	136.10	101.90	133.65	16.55	113.07	59.46	106.59	138.44	301.05	99.81	247.24
aug-cc-pV5Z	23.59	136.57	102.90	134.17	16.60	113.59	60.11	107.03	138.75	301.94	100.07	248.05
cc-pCVDZ	22.83	122.58	82.37	117.58	16.43	97.59	40.57	89.52	130.33	270.96	90.22	214.95
cc-pCVTZ	23.48	132.01	97.52	130.92	17.14	107.48	53.31	100.28	137.15	295.70	97.54	236.45
cc-pCVQZ	23.72	136.18	102.41	134.18	16.90	111.70	57.97	104.40	139.14	301.67	98.61	243.95
cc-pCV5Z	23.77	137.27	104.14	135.10	17.14	113.28	59.48	105.60	139.55	303.43	98.83	246.08
cc-pwCVDZ	22.87	124.64	83.65	118.32	16.57	98.33	41.16	89.31	130.63	271.93	89.64	214.66
cc-pwCVTZ	23.58	133.58	98.91	132.19	17.00	107.95	53.87	100.65	137.76	297.87	97.20	237.15
cc-pwCVQZ	23.75	136.58	102.78	134.43	16.94	111.94	58.07	104.41	139.24	302.08	98.43	244.01
cc-pwCV5Z	23.79	137.46	104.31	135.22	16.95	113.34	59.53	105.62	139.60	303.64	98.78	246.15
aug-cc-pCVDZ	22.92	130.70	86.51	123.22	16.73	109.12	50.39	100.87	132.68	282.39	94.64	236.59
aug-cc-pCVTZ	23.56	134.65	99.28	131.76	17.29	111.80	57.31	103.78	137.61	297.37	98.71	242.51
aug-cc-pCVQZ	23.73	137.11	103.45	134.71	16.96	113.36	59.59	105.78	139.28	302.75	98.94	246.26
aug-cc-pCV5Z	23.78	137.68	104.53	135.31	17.29	113.99	60.18	106.15	139.62	303.83	99.01	247.07
aug-cc-pwCVDZ	22.96	131.30	87.52	124.08	16.93	109.27	50.74	100.51	132.67	283.26	93.76	235.92
aug-cc-pwCVTZ	23.63	135.43	100.39	132.69	17.12	111.82	57.61	103.96	138.14	298.90	98.45	242.84
aug-cc-pwCVQZ	23.76	137.32	103.75	134.88	16.98	113.46	59.58	105.68	139.36	303.00	98.73	246.17
aug-cc-pwCV5Z	23.79	137.78	104.67	135.40	16.99	113.92	60.19	106.14	139.66	303.98	98.98	247.10
ZPE	0.50	1.27	2.08	1.78	0.22	0.76	1.10	1.00	8.11	4.23	5.85	2.03
Experiment[b]	23.86	137 ± 7	104 ± 3	138 ± 2	17.00	114 ± 7	80 ± 6	110 ± 2	149	304 ± 2	–	245 ± 1

[a] The tight *d* basis sets have been used on Na and Mg. Only the n*s* and n*p* electrons are correlated in the cc-pV*n*Z and aug-cc-pV*n*Z calculations, while the $(n-1)s$ and $(n-1)p$ electrons are correlated in addition to the n*s* and n*p* electrons in the rest of the calculations

[b] Ref. [90]. The atomization energy reported by NIST for BeH$_2$ is an estimate in the absence of reliable experimental data

same CBS limit, as expected. Computations of molecular properties including ionization potentials, electron affinities, atomization energies, and enthalpies of formation also demonstrate the necessity of accounting for core-valence correlation, especially for Li and Na.

Finally, the *sp* basis sets in each case have been re-contracted for scalar relativistic Douglas–Kroll calculations, resulting in DK basis sets that reliably recover the effects of scalar relativity at each basis set level.

References

1. Dunning TH Jr (1989) J Chem Phys 90:1007–1023
2. Dunning TH Jr, Peterson KA, Wilson AK (2001) J Chem Phys 114:9244–9253
3. van Mourik T, Dunning TH Jr (1999) Int J Quantum Chem 76:205
4. Wilson AK, van Mourik T, Dunning TH Jr (1996) J Mol Struct (Theochem) 388:339
5. Wilson AK, Woon DE, Peterson KA, Dunning TH Jr (1999) J Chem Phys 110:7667–7676
6. Woon DE, Dunning TH Jr (1994) J Chem Phys 100:2975
7. Woon DE, Dunning TH Jr (1993) J Chem Phys 98:1358–1371
8. Woon DE, Dunning TH Jr (1995) J Chem Phys 103:4572–4585
9. Feller D (1992) J Chem Phys 96:6104–6114

10. Halkier A, Helgaker T, Jørgensen P, Klopper W, Koch H, Olsen J, Wilson AK (1998) Chem Phys Lett 286:243–252
11. Peterson KA, Woon DE, Dunning TH Jr (1994) J Chem Phys 100:7410
12. Karton A, Martin JML (2006) Theor Chem Acc 115:330
13. Lee EC, Kim D, Jurečka P, Tarakeshwar T, Hobza P, Kim KS (2007) J Phys Chem A 111:3446
14. Schwartz C (1962) Phys Rev 126:1015
15. Wilson AK, Dunning TH Jr (1997) J Chem Phys 106:8718–8726
16. Peterson KA, Dunning TH Jr (1995) J Phys Chem 99:3898–3901
17. Kendall RA, Dunning TH Jr, Harrison RJ (1992) J Chem Phys 96:6796–6806
18. Peterson KA (2003) J Chem Phys 119:11099–11112
19. Peterson KA, Figgen D, Goll E, Stoll H, Dolg M (2003) J Chem Phys 119:11113–11123
20. Peterson KA, Shepler BC, Figgen D, Stoll H (2006) J Phys Chem A 110:13877–13883
21. Balabanov NB, Peterson KA (2005) J Chem Phys 123:064107
22. Balabanov NB, Peterson KA (2006) J Chem Phys 125:074110
23. Peterson KA, Figgen D, Dolg M, Stoll H (2007) J Chem Phys 126:124101
24. Peterson KA, Puzzarini C (2005) Theor Chem Acc 114:283
25. Figgen D, Peterson KA, Dolg M, Stoll H (2009) J Chem Phys 130:164108
26. Peterson KA, Dunning TH Jr (2002) J Chem Phys 117:10548–10560
27. DeYonker NJ, Peterson KA, Wilson AK (2007) J Phys Chem A 111:11383
28. de Jong WA, Harrison RJ, Dixon DA (2001) J Chem Phys 114:48
29. Peterson KA, Adler TB, Werner H-J (2008) J Chem Phys 128:084102
30. Weigend F, Köhn A, Hättig C (2002) J Chem Phys 116:3175
31. Yousaf KE, Peterson KA (2008) J Chem Phys 129:184108
32. Yousaf KE, Peterson KA (2009) Chem Phys Lett 476:303
33. Hill JG, Mazumder S, Peterson KA (2010) J Chem Phys 132:054108
34. Peterson KA (2007) Annu Rep Comput Chem 3:195
35. Woon DE, Dunning TH Jr (unpublished)
36. Feller D (1996) J Comp Chem 17:1571–1586
37. Schuchardt KL, Didier BT, Elsethagen T, Sun L, Gurumoorthi V, Chase J, Li J, Windus TL (2007) J Chem Inf Model 47:1045–1052
38. Press WH, Flannery BP, Teukolsky SA, Vetterling WT (1992) Numerical recipes in FORTRAN 77: the art of scientific computing, 2nd edn. Cambridge University Press, Cambridge
39. DeYonker NJ, Cundari TR, Wilson AK (2006) J Chem Phys 124:114104
40. DeYonker NJ, Grimes T, Yockel SM, Dinescu A, Mintz BJ, Cundari TR, Wilson AK (2006) J Chem Phys 125:104111
41. DeYonker NJ, Ho DS, Wilson AK, Cundari TR (2007) J Phys Chem A 111:10776–10780
42. DeYonker NJ, Mintz BJ, Cundari TR, Wilson AK (2008) J Chem Theory Comp 4:328–334
43. DeYonker NJ, Peterson KA, Steyl G, Wilson AK, Cundari TR (2007) J Phys Chem A 111:11269
44. Koput J, Carter S, Peterson KA, Theodorakopoulos G (2002) J Chem Phys 117:1529
45. Koput J, Peterson KA (2002) J Chem Phys 116:9255
46. Koput J, Peterson KA (2003) J Phys Chem A 107:3981–3986
47. Koput J, Peterson KA (2006) J Chem Phys 125:044306
48. Li H, Le Roy RJ (2006) J Chem Phys 125:044307
49. Li H, Le Roy RJ (2007) J Phys Chem A 111:6248
50. Roos B, Salez C, Veillard A, Clementi E IBM Research RJ518 (1968), as modified by TH Dunning, Jr and RM Pitzer
51. Roothaan CCJ, Bagus PS (1963) Meth Comp Phys 2:47
52. H-J Werner, PJ Knowles, R Lindh, FR Manby, M Schütz et al. (2009) MOLPRO, version 2009.1, a package of ab initio programs, see http://www.molpro.net
53. Woon DE, Dunning TH Jr (1992) J Chem Phys 98:1358–1371
54. Bartlett RJ, Stanton JF (1994) In: Lipkowitz KB, Boyd DB (eds) Reviews in computational chemistry, vol 5. VCH Publishers Inc, New York, p 65
55. Purvis GD, Bartlett RJ (1982) J Chem Phys 76:1910–1918
56. Raghavachari K, Trucks GW, Pople JA, Head-Gordon M (1989) Chem Phys Lett 157:479–483
57. Lias SG, Bartmess JE, Liebman JF, Holmes JL, Levin RD, Mallard WG (2005) In: Linstrom PJ, Mallard WG (eds) NIST chemistry webbook, NIST standard reference database number 69. National Institute of Standards and Technology, Gaithersburg
58. Raffenetti RC (1973) J Chem Phys 58:4452–4458
59. Partridge H (1989) J Chem Phys 90:104
60. Huber KP, Herzberg G (1979) Molecular spectra and molecular structure IV. Constants of diatomic molecules. Van Nostrand, Princeton
61. Spitznagel G, Clark T, PvR Schleyer, Hehre WJ (1987) J Comp Chem 8:1109
62. Bauschlicher CW, Partridge H (1995) Chem Phys Lett 240:533
63. Martin JML (1998) J Chem Phys 108:2791–2800
64. Wang NX, Wilson AK (2003) J Phys Chem A 107:6720–6724
65. Bauschlicher CW, Partridge H (1997) Chem Phys Lett 276:47–54
66. Martin JML, Uzan O (1998) Chem Phys Lett 282:16–24
67. Wilson AK, Dunning TH Jr (2003) J Chem Phys 119:11712–11714
68. Wilson AK, Dunning TH Jr (2004) J Phys Chem A 108:3129–3133
69. Wang NX, Wilson AK (2005) J Phys Chem A 109:7189–7196
70. Prascher BP, Lucente-Schultz RM, Wilson AK (2009) Chem Phys 359:1
71. Iron MA, Oren M, Martin JML (2003) Mol Phys 101:1345
72. Kagi E, Hirano T, Takano S, Kawaguchi K (1994) J Mol Spectrosc 168:109
73. Törring T, Hoeft J (1986) Chem Phys Lett 126:477
74. Kagi E, Kawaguchi K (2006) J Mol Struct 795:179–184
75. Mürtz P, Thümmel H, Pfelzer C, Urban W (1995) Mol Phys 86:513
76. Lee TJ, Taylor PR (1989) Int J Quantum Chem Symp 23:199
77. Lorenzen CJ, Niemax K (1982) J Phys B 15:L139–L145
78. Beigang R, Schmidt D, West PJ (1983) J Physics (Paris), Colloquium C7 44:229–237
79. Baugh JF, Burkhardt CE, Leventhal JJ, Bergeman T (1998) Phys Rev A 58:1585
80. Ciocca M, Burkhardt CE, Leventhal JJ, Bergeman T (1992) Phys Rev A 45:4720–4730
81. Chang ES (1987) Phys Scr 35:792–797
82. Kaufman V, Martin WC (1991) J Phys Chem Ref Data 20:83–153
83. Martin WC, Musgrove A, Kotochigova S, Sansonetti JE, (2003) National Institute of Standards and Technology, Gaithersburg. http://www.nist.gov/physlab/data/ion_energy.cfm
84. Wang X, Andrews L (2005) Inorg Chem 44:610–614
85. Yu S, Shayesteh A, Bernath PF, Koput J (2005) J Chem Phys 123:134303
86. Wang X, Andrews L (2004) J Phys Chem A 108:11511
87. Snelson A (1966) J Phys Chem 70:3208
88. Shayesteh A, Tereszchuk K, Bernath PF, Colin R (2003) J Chem Phys 118:3622
89. Shayesteh A, Appadoo DRT, Gordon I, Bernath PF (2003) J Chem Phys 119:7785
90. Chase MW (1998) J Phys Chem Ref Data 9:1